



Using microwave refraction to determine local inhomogeneities of a rotating plasma

Yurii P. Martseniuk ,
Yevhen V. Siusko ,
Yurii V. Kovtun

Abstract. To determine the local inhomogeneities of a rotating plasma, the method based on microwave refraction was used. The method is based on spectral and correlation analysis of the reflected signals from the rotating plasma layer at normal and inclined microwave incidence. This method allowed us to determine local inhomogeneities of plasma electron density, angles of azimuthal displacement of grooves, and its angular frequency of rotation. Using an additional 4th horn antenna, in contrast to previous works, it was possible to find and analyze two regions with azimuthal inhomogeneities in the rotating plasma. Analysis of the reflected signals shows the presence of four grooves, and the angular frequency of rotation $\omega = 1.16 \times 10^4$ rad/s was also determined.

Keywords: Horn antenna • Inhomogeneities • Reflected microwave • Reflectometry • Refraction

Introduction

Plasma in crossed electrical and magnetic fields is attractive for a wide range of physical and applied problems concerning the laboratory, fusion, and space plasmas [1–4]. One of the features of such plasma is its rotation. Under certain conditions, various instabilities may develop in a rotating plasma [2, 4, 5]. The probe method can be used to diagnose plasma inhomogeneities [6, 7]. This is a contact method, and so, it has limitations on plasma density and temperature. The microwave methods which include no contact and at the absence of temperature limitations are good for diagnostics of dense and hot plasmas [8, 9]. To diagnose dense plasma ($N_e \geq 10^{12} - 10^{14} \text{ cm}^{-3}$), methods of microwave plasma reflectometry (including correlation, correlation poloidal, and Doppler reflectometry) are widely used [8–13].

Plasma diagnostics also use methods based on the refraction of microwave rays in plasma [14]. The method for the determining local inhomogeneities of the rotating plasma was proposed in the study by Kovtun and Siusko [15]. Approbation of the method was tested on a mechanical model [15, 16]. The method is based on spectral and correlation analysis of reflected signals from the plasma during normal and oblique microwave probing. Thus, the use of this method allowed us to identify the oscillation

Yu. P. Martseniuk[✉], Y. V. Siusko, Yu. V. Kovtun
Institute of Plasma Physics National Science Center
“Kharkiv Institute of Physics and Technology”
Kharkiv, Ukraine
E-mail: martsenyukY@kipt.kharkov.ua

Received: 22 August 2022
Accepted: 30 January 2023

0029-5922 © 2023 The Author(s). Published by the Institute of Nuclear Chemistry and Technology.
This is an open access article under the CC BY-NC-ND 4.0 licence (<http://creativecommons.org/licenses/by-nc-nd/4.0/>).

of the electron plasma density with the azimuthal mode $m = 3$ and to determine the values of the azimuthal displacement of the grooves and angular frequency. This method is most applicable when the microwave length is smaller than the area of plasma inhomogeneity.

This work is a continuation of the earlier studies [15, 16]. The main goal was to further develop a method for determining local plasma inhomogeneities, expanding its possibilities and informativeness. Four horn antennas were used simultaneously for this purpose. One horn antenna was transmitting and receiving signals, while the other three were only receiving signals. This allowed the analysis of two regions in the rotating plasma, in addition to control more accurately the time interval when the microwave cannot propagate through the plasma column.

Experimental setup

An experimental study of dense multicomponent plasma was carried out on the MAKET facility. The experimental setup is a Penning cell in which high-power pulsed reflex discharge in cross electrical and magnetic fields is realized [17]. A schematic representation of the MAKET facility is shown in Fig. 1. The maximum values of the discharge system parameters are as follows: discharge voltage: 5 kV, pulse time: ~ 4 ms, discharging current: ~ 2 kA, battery capacity: 560 μF , and stored energy: 7 kJ. The magnetic field was generated by a solenoid consisting of six coils. The two end coils produced magnetic mirrors with a mirror ratio of 1.25. The parameters of the magnet mirror discharge system are as follows: discharge voltage: ≤ 3 kV, magnetic induction: ≤ 0.9 T, pulse duration: 18 ms, vacuum chamber volume: $\sim 7 \times 10^4$ cm^3 , plasma volume: $\sim 10^4$ cm^3 , and chamber radius: 10 cm. The radius of the plasma layer with a density above 1.7×10^{15} cm^{-3} is 5 cm [15].

The vacuum chamber was pumped to a pressure of 1.3×10^{-4} Pa; then, Ar working gas was injected into the chamber at a pressure of 0.28–0.96 Pa. The cathodes were made of Ti. The initial voltage of the capacitive storage was set at $U_0 \leq 3.6$ kV; the maximum current was up to 1.2 kA. The electrical discharge was initiated with a delay of 2 ms relative to the magnetic field. Discharge current and voltage were measured by Rogowski coil and voltage divider, respectively. A ballast resistance of $R = 2.6$ Ohm was used to limit the discharge current.

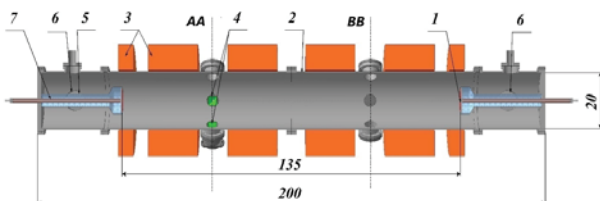


Fig. 1. A schematic image of the experimental MAKET facility. 1 – Cathode; 2 – the vacuum chamber (anode); 3 – the magnetic system; 4 – horn antennas; 5, 7 – insulators; 6 – the vacuum-pumping system; AA, BB – sections of diagnostic ports. (The dimensions in the figure are in cm).

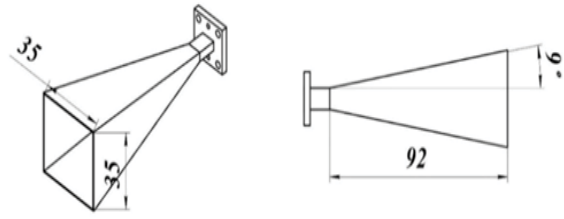


Fig. 2. Geometric parameters of the horn antenna.

Diagnostic techniques

Plasma probing was carried out by an ordinary wave (O-wave) at the frequency range of 38.23 GHz. In the experiments, we simultaneously recorded the transmitted and reflected microwave signals during normal and oblique sounding. Four pyramidal horn antennas were used for transmitting and receiving microwave radiation. The geometric dimensions of the antennas and of the material (stainless steel) from which the antennas are made are identical. Figure 2 shows a picture of the horn antenna installed in the MAKET facility and its geometric dimensions. The size of the cross section of the antenna is as follows: antenna opening: $a b$ 35 mm, axial height: 92 mm, aperture angle: 9° , and the opening of the rectangular waveguide: $a = 7$ mm, $b = 3$ mm.

The arrangement of the horn antennas for the experimental installation is shown in Fig. 3. Antenna 1 was used to transmit and receive microwave radiation. Receiving antennas 2 and 4 were shifted along the azimuth at an angle of $60 \pm 3^\circ$ lower and upper relative to antenna 1. Antenna 3 was shifted by an angle of 180° to antenna 1. The horn antennas in the MAKET facility are installed in the diagnostic ports located in section AA (Fig. 1). Changing the angle of the antennas is not permitted by design. The diagnostic ports are removed at a distance of 50 cm from the ends of the vacuum (discharge) chamber and, respectively, at a distance of 30 cm from the end electrodes (cathodes). Microwave signals were generated by a G4-115 oscillator that can produce output power of up to 20 mW. The frequency error does not exceed 0.1%. The microwave radiation was detected by amplitude detectors (semiconductor microwave

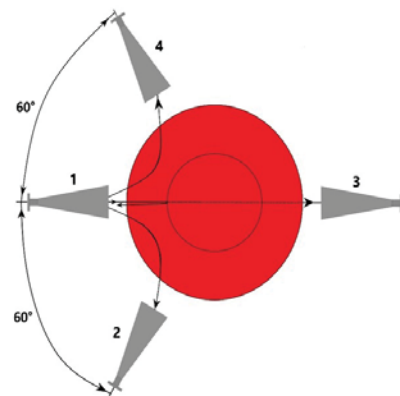


Fig. 3. The arrangement of the horn antennas in the experimental installation. 1 – Receiving and transmitting antenna, 2 – receiving lower antenna, 3 – receiving antenna, 4 – receiving upper antenna.

diodes). The relationship between the input power and the detected output voltage is the square root.

Moreover, the time dependence of the voltage was measured using a high-voltage ohmic divider. The voltage ratio was 921; and the rise time constant was less than 1 μ s. The time dependence of the integral flow of plasma emission from the discharge was registered using the photodetector. The photodetector is manufactured on the basis of the photodiode FDUK-13U and operates in a photodiode mode [17]. The photodiode has a wavelength range of $\lambda = 180 \dots 1100$ nm with a maximum sensitivity at 940 nm [18]. The rise time constant of the signal is ~ 300 ns. It was installed on the surface of a quartz window in one of the ports of the BB section (Fig. 1). The voltage divider and photodetector signals were registered by the oscilloscope Tektronix TDS2014B with a bandwidth of 60 MHz. The microwave signals were registered by the four-channel oscilloscope Hantek DSO3064.

The principle of the diagnostic method to determine local inhomogeneities of a rotating plasma

For describing the principle of the diagnostic method, the geometric optic approximation is used. The plasma is assumed to be a cylindrically layered plasma. The inclined microwave rays which go through the plasma continuously refract; then, they reflect from the critical layer and go supposedly through the same layers, making them move along the same optic path. The amplitude of the microwave signal in the receiver antenna is very sensitive to the inhomogeneities of the critical layer and depends on the distance from the critical layer to the antenna opening. The presence of additional antennas that receive the reflected signal allows us to perform spectral and correlation analysis of the reflected signals. Because the plasma rotates, when you know the period of rotation, it is possible to detect inhomogeneities of the critical layer, their number, and the azimuthal angle of displacement between them and the angular frequency of rotation.

To perform spectral and correlation analysis of reflected microwave signals, we used auto-correlation functions (ACFs) and cross-correlation functions (CCFs) [19]. The correlation (covariance) functions of stationary random processes for arbitrary fixed t and τ_k are defined as follows:

$$(1) \quad R_{AA}(\tau_k) = \frac{1}{N} \sum_{t=0}^{N-1} A(t)A(t + \tau_k)$$

$$(2) \quad R_{12}(\tau_k) = \frac{1}{N} \sum_{t=0}^{N-1} A_1(t)A_2(t + \tau_k)$$

The quantity $R_{AA}(\tau_k)$ is called the ACF of $A_1(t)$, whereas $R_{12}(\tau_k)$ is called the CCF between $A_1(t)$ and $A_2(t)$. N is the number of points in the signal realization, τ_k is the time shifting, and $A(t)$ is the amplitude of the received signals (A_1 or A_2).

The angular frequency of the rotating cylinder can be determined by equation [20–22]:

$$(3) \quad \omega = \Delta\varphi / \Delta\tau, \text{ (rad/s)}$$

where $\Delta\varphi$ is the angular distance between the reception points of the reflected wave (in case of use ACF $\Delta\varphi 2\pi$) and $\Delta\tau$ is the time shift between the maxima of the CCF or the ACF period ($T \Delta\tau$). Also, the aperture angle of the transmitting and receiving antennas to determine the angular distance should be considered. Simultaneous analysis of CCF and ACF allows us to determine the angular frequency of rotation more accurately, allowing us to determine with higher accuracy the presence and number of grooves. When the angular frequency and number of grooves are determined, it is easy to determine their azimuthal displacement angles.

Experimental results and discussion

The experimental results are shown in Fig. 4. Figures 4a and 4b show the time evolution of discharge voltage and plasma optical emission intensity, respectively. A closer look at the time evolution of discharge voltage is shown in Figs. 5a and 5b. The time evolution of the amplitude of the detected microwave signals is shown in Figs. 4c–f. The microwave signal transmitted across the plasma column as shown in Fig. 4c was received by antenna 3 (see Fig. 3). When the critical density $N_{cr} = 1.81 \times 10^{15} \text{ cm}^{-3}$ for frequency 38.23 GHz is reached, the ordinary wave cannot propagate through the plasma column. Accordingly, the amplitude of the signal decreases almost to zero for a time interval from 0.2 ms to 4.7 ms (see Fig. 4c). At the same time, the microwaves will be reflected from the plasma layer with a critical density. Figure 4d shows the reflected signal at normal incidence received by antenna 1. The signals reflected at oblique incidence as shown

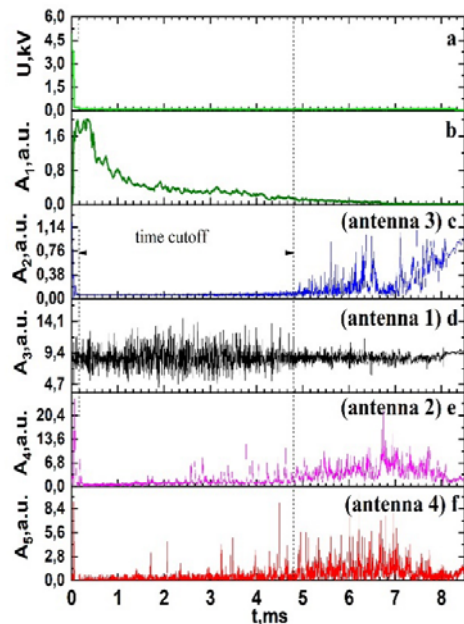


Fig. 4. Time evolution of discharge voltage (a), plasma optical emission intensity (b), (c–f) – amplitudes of detected microwave signals received by antennas 3, 1, 2, and 4 (see Fig. 3) respectively.

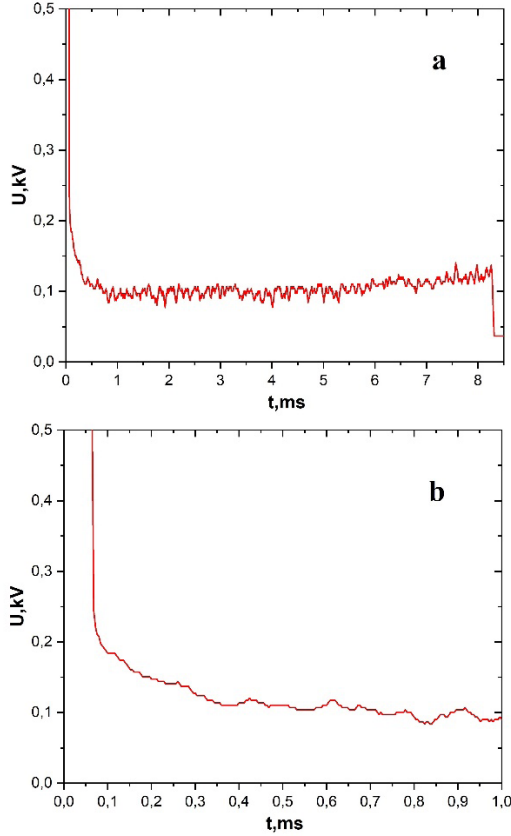


Fig. 5. A closer look at the time evolution of discharge voltage.

in Figs. 4e and 4f were received by antennas 2 and 4, respectively.

By analyzing the signals as in Figs. 4a–c, 5a, and 5b, we can see that in the time interval of about 100 μ s is a breakdown of the gas gap between the cathode and anode in the discharge chamber. In this case, the discharge voltage decreases rapidly up to 200 V (see Figs. 5a and 5b); there is a sharp increase in both plasma density and optical emission, as shown in Fig. 4b. Due to the growth of plasma density above the critical value, the signal as shown in Fig. 4c is cut off. The plasma density increases. The plasma layer with the critical density becomes closer to the antenna, and so, the increase of the amplitude of the reflected signal as shown in Fig. 4d can be seen. At the same time, at the time interval from 0.1 ms to 1.5 ms, a microwave signal as shown in Figs. 4e and 4f on the antennas azimuthally shifted on 60° should also be presented. The absence of signals at this interval is due to the fact that the radius r_{cr} of the plasma layer with the critical density has become so large that due to reflection and refraction some or all of the microwave rays do not reach the receiving horn antennas.

Calculations of the critical radius r_{cr} of the plasma layer [23] with the density N_{cr} , when the rays do not hit the antenna, showed that the value of r_{cr} belongs to the interval from 4.5 cm to 6.5 cm for various functions of the radial distribution of the plasma density [23]. Measurements for r_{cr} with $N_{cr} \geq 1.72 \times 10^5 \text{ cm}^{-3}$ by the reflectometry method, as in [24], have shown that r_{cr} can reach a value of ≈ 5 cm. The

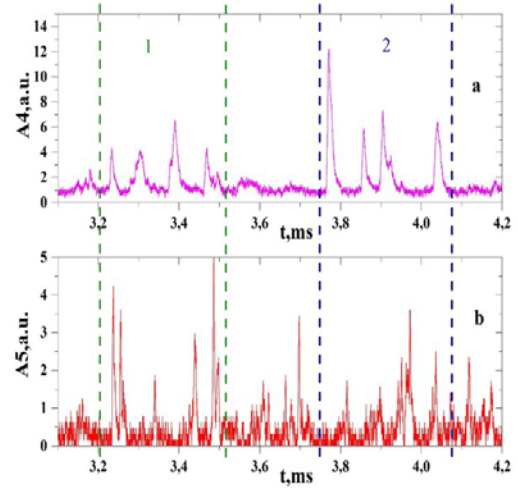


Fig. 6. Oscillograms of the amplitude of detected microwave signals received by antennas: 4 (a), 2 (b) (see Fig. 3).

estimation of the error in these measurements was carried out according to Kovtun *et al.* [25] and amounted to no more than 20%.

In the time interval from 1.5 ms to 4.7 ms, (see Figs. 4e and 4f), we can see the increase in the amplitude of reflected signals received at angles of 60° relative to the antenna 1. The signals on the shifted horn antennas 2 and 4 are related to reflection from the plasma layer and refraction. These signals carry information about the inhomogeneities of the rotating plasma. The reflected signals at angles of 60° starting from 4.7 ms on the one hand are caused by the scattering of microwaves on plasma fluctuations and, on the other hand, by possible reflection from the wall of the discharge chamber.

In the case where the plasma density is $N_p \geq N_{cr}$, the oscillograms of the signals detected at angles of 60° relative to transmitting antenna 1 are shown in Fig. 6. As can be seen from Fig. 6, a periodic change in the amplitude of the microwave signals is observed, and these maxima shifted relative to each other in time. In this case, the periodic change in time of the amplitude of the signal received by the antennas (see Fig. 6) is due to the fact that microwave rays hit or miss the receiving antennas. Accordingly, the radius of the reflecting plasma layer changes in the azimuthal direction. As the plasma rotates, there is a periodic change in the amplitude of the received signal. A similar pattern was observed earlier for plasma [15] and for the mechanical model [15, 16]. The shape and amplitude of microwave signals (see Fig. 6) received by antennas 2 and 4 significantly depend on the presence or absence of grooves on the cylinder surface and their geometric dimensions. Conventionally in Fig. 6, we can distinguish two zones. Zones 1 and 2 are showing local density inhomogeneities in the plasma. The analysis of the reflected signals shows the presence of four plasma grooves. We suppose that the radial size of the grooves is about 1 cm. This value is more than the probing wavelength. According to this condition, the application of the method to determine local inhomogeneities is correct. According to the ACF of the reflective signals, the angular frequency is

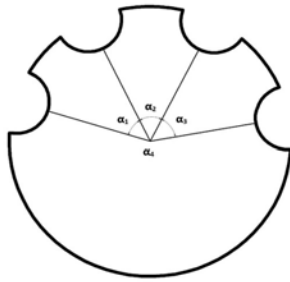


Fig. 7. Sketch illustrating layers with critical density with azimuthal inhomogeneities $\alpha_1 - 47^\circ$, $\alpha_2 - 53^\circ$, $\alpha_3 - 53^\circ$, $\alpha_4 - 207^\circ$.




$\omega = 1.16 \times 10^4$ rad/s. Since the amplitude of the signals increases first at the receiving antenna 4 and then at antenna 2, the inhomogeneities move in the direction from antenna 4 to antenna 2. Accordingly, the plasma rotates anticlockwise in Fig. 3. The value of the azimuthal displacement of the grooves is $\approx 47^\circ$, 53° , 53° , and 207° . The presence of plasma inhomogeneity seems to be associated with the development of plasma instability in crossed fields. Figure 7 is a sketch that illustrates layers with critical density and azimuthal inhomogeneities and the displacement angles between them. The real situation may be more complicated. Between zones 1 and 2 in Fig. 6b, the signal amplitude periodically increases. At the same time, there is practically no change in the amplitude in Fig. 6a. This may be due to changes on the reflective layer (groove formation) as the plasma is rotating from antenna 4 to antenna 2. When using in this experiment, one pair of antennas, such as 1 and 4, it would be impossible to see these changes. And conversely using only antennas 1 and 2, these changes were observed. Accordingly, the use of three antennas made it possible to analyze two regions in the rotating plasma. This allowed us to identify local inhomogeneities that change weakly during one revolution of the plasma around the axis.

Conclusions

Four horn antennas were used simultaneously in the experiments. One horn antenna was transmitting and receiving signals, while the other three were only receiving. This allowed two regions in the rotating plasma to be analyzed to control more accurately the time interval when the microwave cannot propagate through the plasma column. The analysis of the reflected signals shows the presence of inhomogeneities plasma density. Four grooves shifted along the azimuth were determined. The azimuthal displacement angles of the grooves are $\approx 47^\circ$, 53° , 53° , and 207° . Also, the angular frequency of rotation, which is $\omega = 1.16 \times 10^4$ rad/s, was determined. The presence of plasma inhomogeneity seems to be associated with the development of plasma instability in crossed fields. It should be noticed that this method can be used together with microwave plasma reflectometry. This will provide additional information about the investigated plasma.

Acknowledgment. This work has been carried out within the framework of the EUROfusion Consortium, funded by the European Union via the Euratom Research and Training Programme (Grant Agreement No. 101052200 – EUROfusion). Views and opinions expressed are however those of the author(s) only and do not necessarily reflect those of the European Union or the European Commission. Neither the European Union nor the European Commission can be held responsible for them. Work was performed under EUROfusion WP EDU.

ORCID

Yu. V. Kovtun  <http://orcid.org/0000-0003-4948-0896>
 Yu. P. Martseniuk  <http://orcid.org/0000-0002-2574-7325>
 Y. V. Siusko  <http://orcid.org/0000-0002-0789-7100>

References

- Lehnert, B. (1971). Rotating plasmas review paper rotating plasmas. *Nucl. Fusion*, 11(5), 485. <http://iopscience.iop.org/0029-5515/11/5/010>.
- Boeuf, J. -P. (2014). Rotating structures in low temperature magnetized plasmas – insight from particle simulations. *Front. Physics*, 2, 74. <https://doi.org/10.3389/fphy.2014.00074>.
- Boeuf, J. -P., & Smolyakov, A. (2018). Preface to special topic: Modern issues and applications of $E \times B$ plasmas. *Phys. Plasmas*, 25(6), 061001. <https://doi.org/10.1063/1.5040848>.
- Kaganovich, I. D., Smolyakov, A., Raites, Y., Ahedo, E., Mikellides, I. G., Jorns, B., Taccogna, F., Gueroult, R., Tsikata, S., Bourdon, A., Boeuf, J. -P., Keidar, M., Powis, A. T., Merino, M., Cappelli, M., Hara, K., Carlsson, J. A., Fisch, N. J., Chabert, P., Schweigert, I., Lafleur, T., Matyash, K., Khrabrov, A. V., Boswell, R. W., & Fruchtman, A. (2020). Physics of $E \times B$ discharges relevant to plasma propulsion and similar technologies. *Phys. Plasmas*, 27(12), 120601. <https://doi.org/10.1063/5.0010135>.
- Lucken, R., Bourdon, A., Lieberman, M. A., & Chabert, P. (2019). Instability-enhanced transport in low temperature magnetized plasma. *Phys. Plasmas*, 26(7), 070702. <https://doi.org/10.1063/1.5094422>.
- Gravier, E., Brochard, F., Bonhomme, G., Pierre, T., & Briançon, J. L. (2004). Low-frequency instabilities in a laboratory magnetized plasma column. *Phys. Plasmas*, 11(2), 529–537. <https://doi.org/10.1063/1.1636479>.
- Lockwood Estrin, F., Karkari, S. K., & Bradley, J. W. (2017). Triple probe interrogation of spokes in a HiPIMS discharge. *J. Phys. D-Appl. Phys.*, 50(29). <https://doi.org/10.1088/1361-6463/aa7544>.
- Hartfuss, H. J., & Geist, T. (2013). *Fusion plasma diagnostics with mm-waves: An introduction*. Hamburg: Wiley.
- Mazzucato, E. (2014). *Electromagnetic waves for thermonuclear fusion research*. World Scientific Publishing.
- Conway, G. D. (2006). Microwave reflectometry for fusion plasma diagnosis. *Nucl. Fusion*, 46(9), S665. <https://doi.org/10.1088/0029-5515/46/9/S01>.

11. Grekov, D. L., & Tretiak, K. K. (2017). Investigation of dual polarization reflectometry for determination of plasma density and magnetic field in a spherical tokamak. *J. Fusion Energy*, 36(1), 1–8. <https://doi.org/10.1007/s10894-016-0114-x>
12. Pavlichenko, O. S., Skibenko, A. I., Fomin, I. P., Pinos, I. B., Ocheretenko, V. L., & Berezhniy, V. L. (2000). A simple method of poloidal rotation velocity measurement in toroidal plasmas via microwave reflectometry. *Probl. At. Sci. Technol.*, 6, 172–174.
13. Prisiazhniuk, D., Krämer-Flecken, A., Conway, G. D., Happel, T., Lebschy, A., Manz, P., Nikolaeva, V., & Stroth, U. (2017). Magnetic field pitch angle and perpendicular velocity measurements from multi-point time-delay estimation of poloidal correlation reflectometry. *Plasma Phys. Control. Fusion*, 59(2), 025013. <https://doi.org/10.1088/1361-6587/59/2/025013>.
14. Siusko, Y. V., & Kovtun, Yu. V. (2021). An application of microwaves refraction for inhomogeneous plasma diagnostic. *Probl. At. Sci. Technol.*, 2, 163–170. <https://doi.org/10.46813/2021-131-163>.
15. Kovtun, Yu. V., & Siusko, Y. V. (2019). Determining local inhomogeneities of rotating plasma density via microwave refraction. *Phys. Lett. A*, 383(31), 125880. <https://doi.org/10.1016/j.physleta.2019.125880>.
16. Kovtun, Y., & Siusko, Y. (2020). Determining the angular frequency of rotating cylinder via microwave. In 2020 IEEE Ukrainian Microwave Week, UkrMW 2020 – Proceedings (pp. 888–892). DOI: 10.1109/UkrMW49653.2020.9252707.
17. Kovtun, Y. V., Shapoval, A. N., & Siusko, Y. V. (2019). Observation of multiply charged states ions in a high-power pulsed reflex discharge. *Plasma Sources Sci. Technol.*, 28(10), 105009. <https://doi.org/10.1088/1361-6595/ab46c8>.
18. Kovtun, Yu. V., Skibenko, A. I., Skibenko, E. I., Larin, Yu. V., & Yuferov, V. B. (2009). Emission of multicomponent plasma pulsed reflex discharge. *Bulletin of the National Technical University “KhPI” Series “High voltage engineering and electrophysics”*, 39, 101–108.
19. Shanmugan, K. S., & Breipohl, A. M. (1988). *Random signals, detection, estimation and data analysis*. Hoboken: Wiley.
20. Kovtun, Yu. V., & Siusko, Y. V. (2018). Determining local inhomogeneities of the rotating plasma density via microwave refraction. In International Conference–School on Plasma Physics and Controlled Fusion. Books of abstract, September 10–13, 2018 (p. 175). Kharkiv, Ukraine.
21. Bendat, J. S., & Piersol, A. G. (2011). *Random data: analysis and measurement procedures*. John Wiley & Sons.
22. Kovtun, Yu. V., Skibenko, E. I., Skibenko, A. I., & Yuferov, V. B. (2013). Rotation of plasma layers with various densities in crossed $E \times B$ fields. *Ukr. J. Phys.*, 58(05), 450–457. <https://doi.org/10.15407/ujpe58.05.0450>.
23. Kovtun, Yu. V., Syusko, Y. V., Skibenko, E. I., & Skibenko, A. I. (2018). Experimental study of inhomogeneous reflex-discharge plasma using microwave refraction interferometry. *Ukr. J. Phys.*, 63(12), 1057. <https://doi.org/10.15407/ujpe63.12.1057>.
24. Kovtun, Yu. V., Skibenko, E. I., Skibenko, A. I., & Yuferov, V. B. (2013). Rotation of plasma layers with various densities in crossed $E \times B$ fields. *Ukr. J. Phys.*, 58, 450.
25. Kovtun, Yu. V., Skibenko, A. I., Skibenko, E. I., & Yuferov, V. B. (2013). Analysis of errors in the plasma rotation velocity measurement by the method of microwave correlation reflectometry. In 2013 International Kharkov Symposium on Physics and Engineering of Microwaves, Millimeter and Submillimeter Waves (pp. 554–556). <https://doi.org/10.1109/MSMW.2013.6622119>.